

CHARACTERIZATION OF DEFECTS IN DEUTERIUM-IMPLANTED BERYLLIUM

R. A. Anderl and A. B. Denison

Idaho National Engineering Laboratory
Idaho Falls, Idaho 83415-7113

S. Szpala, P. Asoka-Kumar, K. G. Lynn and B. Nielsen

Brookhaven National Laboratory
Upton, New York 11973-5000

Paper to be published in the Proceedings
of

Fifth International Conference
Hydrogen Effects on Material Behavior

Jackson Lake Lodge, Moran, WY
September 11-15, 1994

DISCLAIMER

This report was prepared as an account of work sponsored by an agency of the United States Government. Neither the United States Government nor any agency thereof, nor any of their employees, makes any warranty, express or implied, or assumes any legal liability or responsibility for the accuracy, completeness, or usefulness of any information, apparatus, product, or process disclosed, or represents that its use would not infringe privately owned rights. Reference herein to any specific commercial product, process, or service by trade name, trademark, manufacturer, or otherwise does not necessarily constitute or imply its endorsement, recommendation, or favoring by the United States Government or any agency thereof. The views and opinions of authors expressed herein do not necessarily state or reflect those of the United States Government or any agency thereof.

MASTER

DISTRIBUTION OF THIS DOCUMENT IS UNLIMITED

amp

DISCLAIMER

Portions of this document may be illegible in electronic image products. Images are produced from the best available original document.

CHARACTERIZATION OF DEFECTS IN DEUTERIUM-IMPLANTED BERYLLIUM

R. A. Anderl and A. B. Denison

Idaho National Engineering Laboratory
Idaho Falls, Idaho 83415-7113

S. Szpala, P. Asoka-Kumar, K. G. Lynn and B. Nielsen

Brookhaven National Laboratory
Upton, New York 11973-5000

Abstract

This work investigated surface material modifications in high-purity beryllium foils resulting from 1-keV deuterium ion implantation into specimens for which the anneal temperatures and implantation temperatures were varied. Defects in unimplanted and in deuterium-implanted beryllium were characterized principally by positron-beam depth-profile analyses. Depth-profiles of the defect distributions in the specimens were made by stepping the energy of the positron beam from 0.055 keV to 40 keV, accompanied by measurements of the Doppler-broadened annihilation radiation line shape at each positron energy. These analyses identified a varying defect structure in beryllium, dependent on the previous anneal history of the material and on the temperature of the material during implantation with energetic deuterium ions. For specimens implanted at room temperature with 1-keV/D ions, the beam-induced defect structure had a profile that was peaked near the mean range of the implanting deuterium and that extended beyond the implantation zone. Isochronal step-thermal anneal experiments revealed that deuterium was released from these defects at a temperature of about 400K, indicative of shallow traps, and that the defect structure annealed at temperatures above 623K. The beam-induced vacancy-defect complexes were estimated to be 1-nm voids for 1-keV/D implantation into Be at room temperature. For beryllium implanted at temperatures of 723K with 1-keV/D ions, these measurements revealed that the beam-induced defect structure was much broader and extended far beyond the implantation zone. Isochronal step-thermal anneal experiments for these specimens revealed a more stable defect structure, with the onset of defect annealing at 775K. There was no evidence of deuterium release at lower temperatures, indicating that for beryllium implanted at elevated temperatures, deuterium is retained in deep traps. These measurements indicated that, for beryllium implanted at elevated temperatures, the beam-induced defects most likely consist of large stable voids with defect concentrations less than that for material implanted at room temperature.

INEL work supported by the U. S. Department of Energy, Office of Energy Research, under DOE Idaho Operations Office Contract DE-AC07-94ID13223. BNL work supported by the DOE Office of Basic Energy Sciences, Division of Materials Sciences, under Contract No. DE-AC02-76CH00016.

Introduction

Present concepts for the International Thermonuclear Experimental Reactor (ITER)[1] include the use of beryllium as a plasma-facing material. As noted by Wilson et al.[2], and references therein, there is disagreement in the literature concerning those parameters that govern the transport, retention and release behavior for hydrogen in Be, namely, diffusivity, solubility, defect trapping, surface molecular recombination and blistering phenomena. The purpose of this paper is to report new experimental information that relates to defect trapping and ion-beam-induced surface modifications that affect hydrogen-isotope retention and permeation in Be. This work focuses on a characterization of defects in unimplanted and deuterium-implanted beryllium foil specimens using positron-beam depth-profile analyses[3].

Much of the earlier work to characterize defects and defect-trapping in Be entailed scanning electron microscopy (SEM) and thermal-desorption mass spectrometry. Anderl et al.[4], in experiments with 3-keV, D_3^+ ions, (1-keV/D), used SEM analyses to determine that, for Be heated to 750K and implanted to a fluence of $2E24$ D/m², the implanted region had a modified surface structure that was textured and pocketed, with interconnected voids. This modified structure, due to vacancy agglomeration, void growth and deuterium bubble formation, extended into the bulk a distance of about 1 μ m, much more than the range for 1-keV D. Deuterium trapping at beam-induced defects was estimated to have a binding energy of 1.5 to 1.8 eV, with deuterium retained in the Be at a maximum concentration of 0.1% between 0.2 and 0.4 μ m. In more recent work, Touhouche and Terreault[5] used SEM analyses to characterize the surface microstructure of beryllium implanted with 1.5-keV deuterium ions with fluences ranging from $3E20$ to $1.2E22$ D/m² and specimen temperatures ranging from 293K to 983K. For specimens heated to temperatures above 473K and for fluences greater than $1.8E21$ D/m² (saturation fluence), the implantation created interconnected blisters that were larger than those for lower temperature implants. At temperatures below 473K, the surface structure exhibited smaller blisters that were not ruptured. In further work, Terreault et al.[6] reported the results of a multi-technique study employing laser-induced, gas-desorption measurements and in-situ annealing measurements in a transmission electron microscope (TEM) to analyze beryllium specimens heated from 300K to 983K and implanted with H and D ions. Pulsed-laser annealing of Be implanted with H(D) at H/Be <14% yielded a value of 1.7 eV for H trapping in Be, and, for H/Be >14%, the trapping energy was 1.0 to 1.2 eV. Surface microstructural modifications in the form of blisters have been reported by Verbeek and Eckstein[7], Liu[8], and Kawamura et al.[9] for high-fluence implantation of deuterium into beryllium. Using thermal-desorption and nuclear-reaction-analysis(NRA) techniques, Wampler studied retention/release mechanisms for deuterium implanted into Be [10,11]. He identified both 1-eV and 1.8-eV trap sites and postulated the precipitation of deuterium bubbles in beryllium implanted with deuterium. Finally, the elastic recoil detection, ion-beam analysis technique was used by Leblanc and Ross[12] to measure ranges of 0.2-keV to 1.0-keV D implanted in Be. This work indicated that the measured ranges were significantly greater than range values predicted using simulation codes like TRIM-92,[13].

Experimental Details

The emphasis of this work was on positron-beam depth-profile analyses to characterize defects in beryllium foil specimens as a function of specimen anneal condition, specimen temperature during implantation, and ion-beam energy and flux. A brief description of the Be specimens, the implantation conditions, and the positron-beam depth-profile technique are presented in this section.

Specimen Description and Preparation

All specimens were made from high-purity beryllium foil obtained from Electrofusion, a Brush-Wellman beryllium special products firm. The foil material, classified as type IF-1, is produced by extruding and hot-rolling an ingot metallurgy cast material that is obtained from vacuum-melted, electrolytically-refined beryllium flakes. Nominal purity of the foil is stated as 99.96% Be with 0.023% C as the main impurity. Both sides of the as-received foil, with a nominal thickness of 100 μm , were mechanically polished to remove the "rough", thick oxide coating that results during fabrication. Finished foil thicknesses were about 70 μm . A polished foil had a nominal surface oxide thickness of about 30 to 40 angstroms before any heat treatment. Heat treatment, even in a high quality vacuum environment, (10^{-5} Pa to 10^{-6} Pa), caused this oxide layer to grow in thickness for temperatures above 673K.

Specimen Implantation with Deuterium

Implantations were made using mass-analyzed D_3^+ ion beams in a system described previously[14,15]. Specimens were implanted with deuterium, for varying specimen temperatures and beam energies. Typical implantation fluxes were about $5\text{E}19$ $\text{D}/\text{m}^2\text{-s}$. Three specimens, Be 4-1, Be 4-4, and Be 4-5, were implanted to a fluence of $2\text{E}24$ D/m^2 with a 3-keV D_3^+ ion beam(1-keV/D). Be 4-1 was annealed and implanted at 723K. Specimen Be 4-4 was not annealed but was implanted at 300K. Be 4-5 was annealed at 723K and implanted at 300K. A fourth specimen, Be 4-2, was annealed at 723K and implanted at 750K to a fluence of $2\text{E}23$ D/m^2 with a 1-keV D_3^+ ion beam(330-eV/D). Specimen Be 4-6 was not annealed or implanted.

Positron-Beam Depth-Profile Analyses

Characterization of the defects in the near surface region of both unimplanted and deuterium-implanted beryllium was achieved using a positron-beam system at the Brookhaven National Laboratory. The application of positron-beam and positron-annihilation spectroscopy(PAS) to study defects in metals has been reviewed in some detail by Schultz and Lynn[3] and by Siegel[16]. A brief description of the technique is given in the following paragraphs.

Use of positrons to characterize defects in solids hinges on unique properties of the positron as it interacts with the solid. Energetic positrons that are implanted into a metal lose energy by scattering, resulting in thermalized positrons with an implantation profile that is dependent on the initial positron energy and on specific properties of the material. A thermalized positron diffuses in the material and eventually annihilates with an electron, resulting in two 511-keV gamma rays that are emitted nearly collinearly but in opposite directions. Measured PAS signatures,(annihilation lifetime, angular correlation between the 511-keV gamma rays, and the shape of the Doppler-broadened annihilation radiation peak), are all sensitive to the specific material and to the electron density of the site at which the positron annihilates. Both the angular correlation between the 511-keV gamma rays and the width of the annihilation radiation peak are sensitive to momentum distributions of the electrons with which the thermalized positrons annihilate. Because the positron can be trapped in localized, bound states in a variety of vacancy-like defects, it becomes a very sensitive probe of defect regions that have significantly lower-than-average electron density, like vacancies, small vacancy clusters, and voids. Hence, because of differences in the PAS signatures between defected and perfect lattices, (longer lifetime, angular correlation spectra and narrower annihilation radiation line shape for defected material), PAS provides important information regarding both the concentration and defect-specific nature of vacancy-like ensembles in metals[16,17].

In the positron-beam depth-profile analyses that were done for beryllium specimens, the characteristic PAS signature that was measured was the Doppler-broadened, annihilation-radiation line shape. Radiation measurements were made with a Ge detector and the Gaussian-like lineshape was analyzed by computing S , a line-shape parameter corresponding to the ratio of counts in the central portion of the annihilation photopeak to the total counts in the peak. S values provide a measure of the relative number of positron annihilations with conduction and core electrons. Positrons trapped at defects are more likely to annihilate with low-momentum conduction electrons, while positrons in perfect crystals tend to annihilate with high-momentum atomic core electrons. Thus Doppler-broadening of the line shape is less in the former and greater in the latter case. S is approximately 0.5 for a defect-free metal, and it can increase by as much as 20% for a metal with defects. A depth-profile of the defect distribution in a specimen was made by stepping the energy of the positron beam from 0.055 keV to 40 keV, accompanied by measurements of the annihilation-radiation lineshape at each positron energy. The positron energies corresponded to mean depths in beryllium ranging from 0.1 nm (the surface) to 0.9 μm . Evolution of the specimen defect structure was monitored by isochronal anneal experiments in which depth-profile S -parameter measurements at room temperature were made following each anneal step.

Measurements and Results

Information on defect distributions in Be was obtained from positron-beam depth-profile analyses described above. In the results presented here the S -parameter data are normalized to bulk or nearly defect-free S -parameter values. With this convention, an S -value of 1 corresponds to a defect-free region, and S -values greater than 1 correspond to regions with defects that are sensitive to positron trapping. A detailed analysis of the positron-beam experiments, to provide specific defect size and concentration, requires a solution of a diffusion/annihilation kinetic equation using the positron implantation profile as the initial condition. Only limited analyses of this type were done.

A comparison of the normalized S -parameter data for all of the deuterium-implanted specimens studied, namely, specimens Be 4-1, 4-2, 4-4, and 4-5, is shown in Figure 1. The S -parameter data are plotted both as a function of positron energy (bottom x-axis) and against the corresponding mean positron depth in nm (top x-axis). The line $S=1$ corresponds to a nearly defect-free region. In the figure, the letters "F" and "B" associated with a specimen identification number indicate whether the analysis was done on the front (beam-interaction) side or on the back side. These data indicate graphically that the defect distributions in the beryllium specimens are very dependent on specimen heat treatment and on the specimen conditions for D implantation.

We first compare the results for Be 4-4 and Be 4-5. For specimen Be 4-4, (no anneal, implant at 300K), there are two peaks in the S -parameter distribution, a narrow one located at a depth close to the range of implanting D and a broad distribution that extends deep into the bulk. In contrast, specimen Be 4-5, (annealed at 723K, implanted at 300K), exhibits only the narrow peak centered near the D range. The narrow peaks in the S -parameter values for Be 4-4 and Be 4-5 correspond closely to one another and are due, primarily, to positrons annihilating in beam-induced defects in that region of the samples. The deeper distribution for Be 4-4 is due most likely to positrons annihilating with defects (vacancies and small vacancy clusters) that result from fabrication processes for the unannealed foil. Annealing of Be 4-5, prior to implantation, eliminated the broad distribution of deep defects for this sample. Measurements (not shown here) for Be 4-6, an unimplanted specimen of beryllium, also indicated a broad distribution in S -parameter values for the unannealed state and a disappearance of the broad distribution after the specimen was annealed to temperatures above 473K. However, Be 4-6 retained a relatively

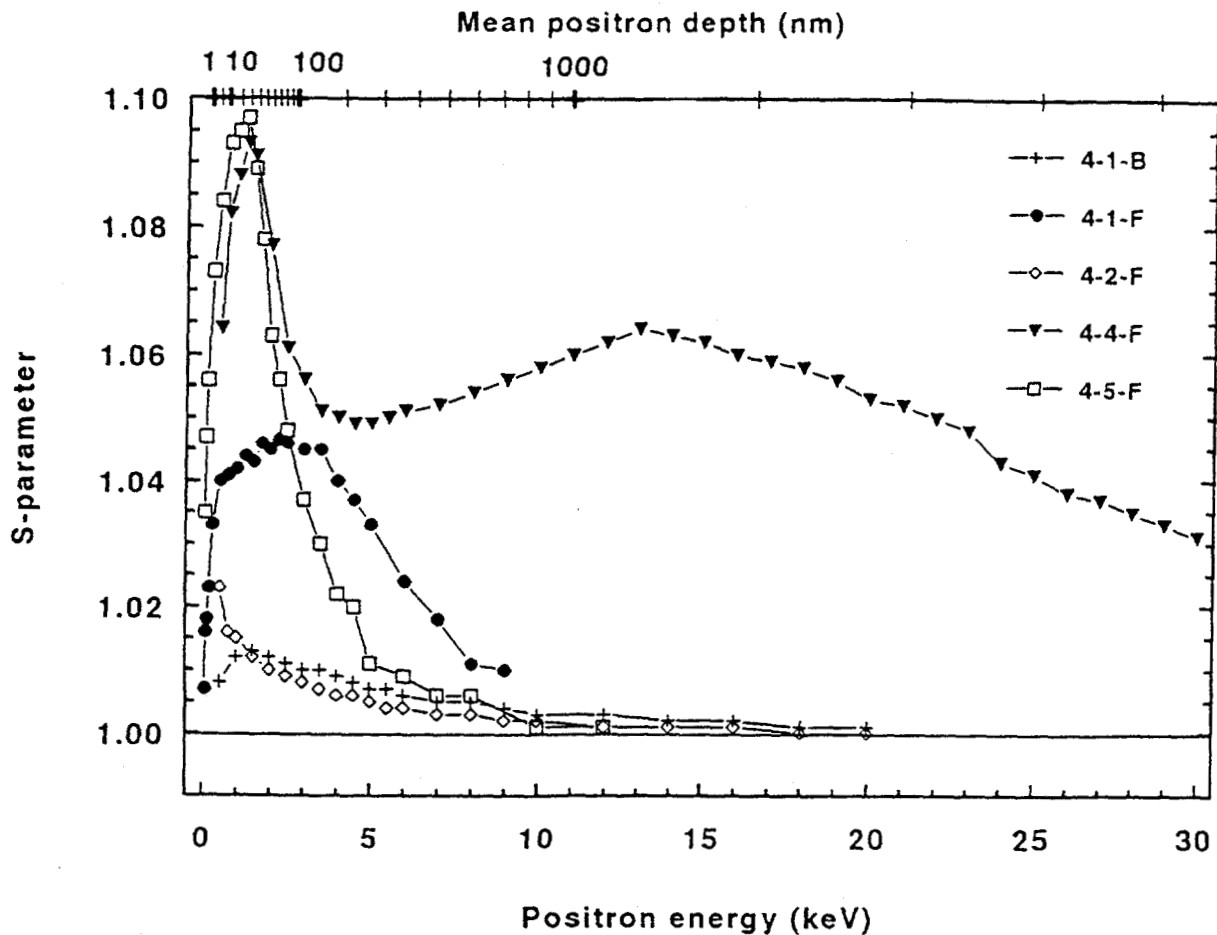


Figure 1. Comparison of S-parameter depth-profile data for unimplanted and deuterium-implanted beryllium foils.

stable, near-surface, defect structure, as was evidenced by a smaller S-parameter distribution that peaked with a value of 1.025 at about 10 nm, even after the specimen was annealed to 973K.

The large narrow S-parameter distributions for Be 4-4 and Be 4-5 provide information related to the range and damage profiles for D that is implanted into Be. For these implantations with 1-keV/D ions, TRIM-92 calculations predict a mean range of 16 nm. The corresponding calculated damage distribution peaks lower in energy than this. We note that the peaks in the S-values for Be 4-4 and 4-5 align with a mean positron depth between 20 and 30 nm. Since the S-value distributions reflect the defect distributions, these measurements indicate that the observed damage distributions peak deeper and are broader than corresponding distributions predicted with TRIM-92. These observations are consistent with the recent measurements of Leblanc and Ross[12], for which the mean range of 1-keV D was determined to be about 30 nm in Be.

Data are also presented in Figure 1 for specimen Be 4-1 that was implanted at an elevated temperature with 1-keV/D ions. Both the front-side and the backside of Be 4-1 were analyzed. A significant difference in front and backside S-value distributions is shown, indicating changes in the defect structure due to implantation of energetic D. The S-value profile for the backside of Be 4-1 peaks near the surface and is similar in magnitude and shape to the S-value distribution observed for annealed Be 4-6 that was never implanted. In contrast, the S-parameter distribution for the beam-interaction side of Be 4-1 is of much greater magnitude than the backside, and the

distribution is much broader than either the backside profile or the profile for Be 4-5, that was annealed but implanted at room temperature. The front-side profile reflects a defect distribution that extends far beyond the implantation zone, an observation that indicates significant vacancy transport and vacancy clustering beyond the implantation zone for beryllium implanted with energetic deuterium, while at an elevated temperature. We note that the magnitude of the S-profile for Be 4-1 is not as large as that for Be 4-5. This could be due to a high concentration of vacancies and small vacancy clusters in the beam-interaction zone for specimens implanted at room temperature (like Be 4-5), whereas, in specimens implanted at elevated temperature (like Be 4-1), vacancies are transported from the beam-interaction zone deeper into the bulk and these vacancies form large volume voids that may contain deuterium gas. Hence, for Be 4-1, the concentration of defects may be smaller and the defect structure may contain larger volume defects, relative to that for Be 4-5, both features that could account for the observed differences in the S-profiles.

Positron depth-profile measurements for Be 4-2, implanted at 753K with 330-eV/D ions, are also shown in Figure 1. The S-profile for this sample peaks much nearer to the surface, reflecting the shorter range for 330-eV ions. Its magnitude is significantly less than that for the other specimens, possibly due to the loss of beam-induced vacancies to the surface during implantation or to limitations of the positron technique for defect profiling so near the surface.

Isochronal anneal measurements were done for specimens Be 4-5 and Be 4-1 from room temperature to 973K. This entailed heating the specimen in steps to successively higher temperatures (e.g., 25K steps for Be 4-5) followed by cooling to room temperature and positron depth-profile measurements. The results of such analyses are shown in Figure 2, with the data for Be 4-5 at the top and that for Be 4-1 at the bottom. Normalized S-parameter data are plotted as a function of anneal temperature. The families of curves shown represent S-values corresponding to the mean positron depths in the material as indicated in the figure. For Be 4-5, the 18-nm depth corresponds to the peak region in the S-value profile, as shown in Figure 1. Similarly, for Be 4-1, the 36-nm and 151-nm depths correspond to the broad peak in the S-value profile shown in Figure 1. Caution should be used in interpreting the anneal data for the surface and 6-nm depths, because these S-values may be significantly influenced by changing surface conditions that affect the positron annihilation signature. Although the S-parameter data for deeper locations are also affected, the influence diminishes the deeper we scan.

We first assess the experiment for Be 4-5 and focus on the trends in the data for 18 nm, 59 nm and 116 nm. There are two significant features in the families of S-parameter as a function of temperature. We observe that the S-values rise abruptly at a temperature between 400K and 425K and they begin to fall off at a temperature near 625K. The rise in S-values at 400K is most likely due to deuterium that is released from shallow trapping sites. This effect could be due to the release of deuterium as D₂ gas inside the voids. Such deuterium is bound less strongly than D at the void wall. This effect has been observed for H in voids in Mo [17]. As discussed by Van Veen[18], an increase in S can indicate the creation of open-volume defects as the deuterium leaves the vacancy-defect traps. Between 425K and 625K, the defect structure is somewhat stable, although the rise in the S-values for the 59-nm and 116-nm depths could indicate further release of deuterium and clustering of mobile defects. The drop in S-values at 625K corresponds to the onset of defect annealing that continues up to temperatures near 825K, with possible further release of deuterium from deeper trap sites. The temperatures at which the defects release deuterium and at which extensive annealing begins are consistent with thermal desorption data from Wampler[11] for beryllium implanted under conditions similar to those here. Maximum S-values observed correspond to defect clusters that are approximately 1-nm voids.

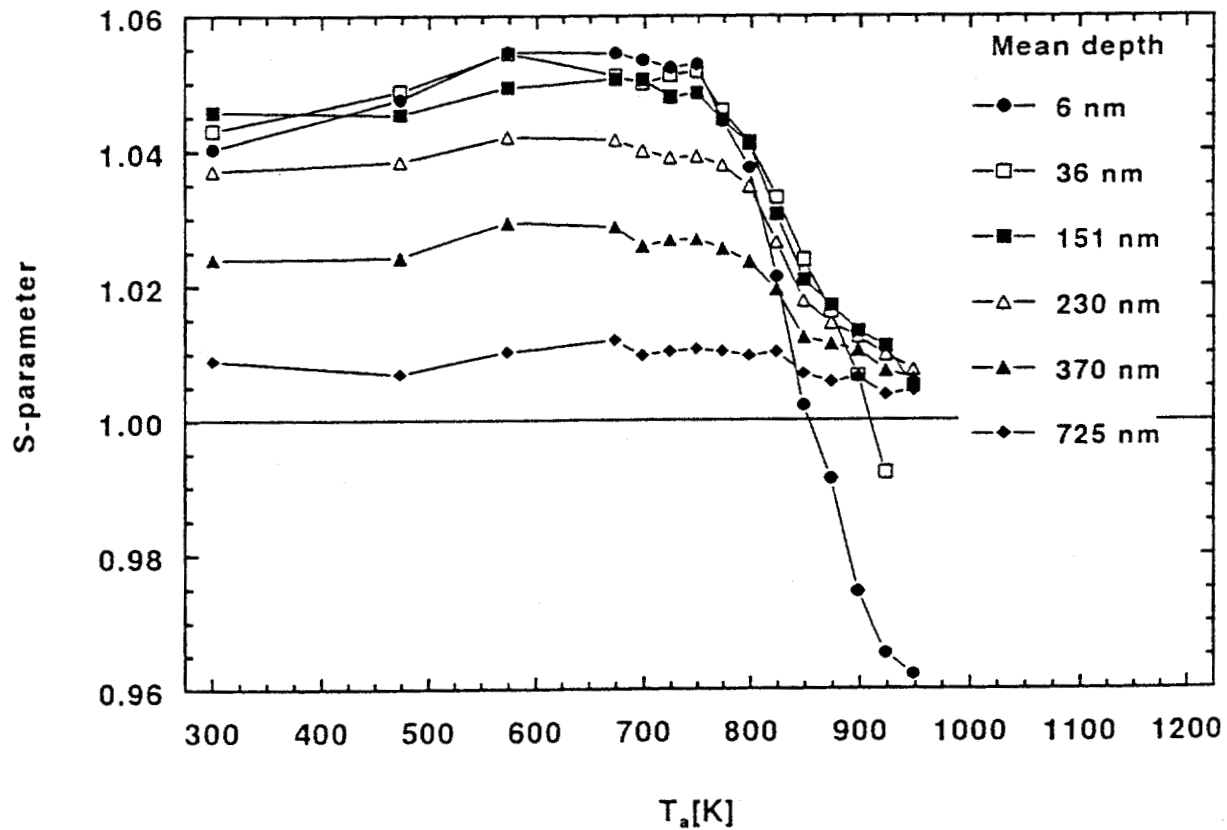
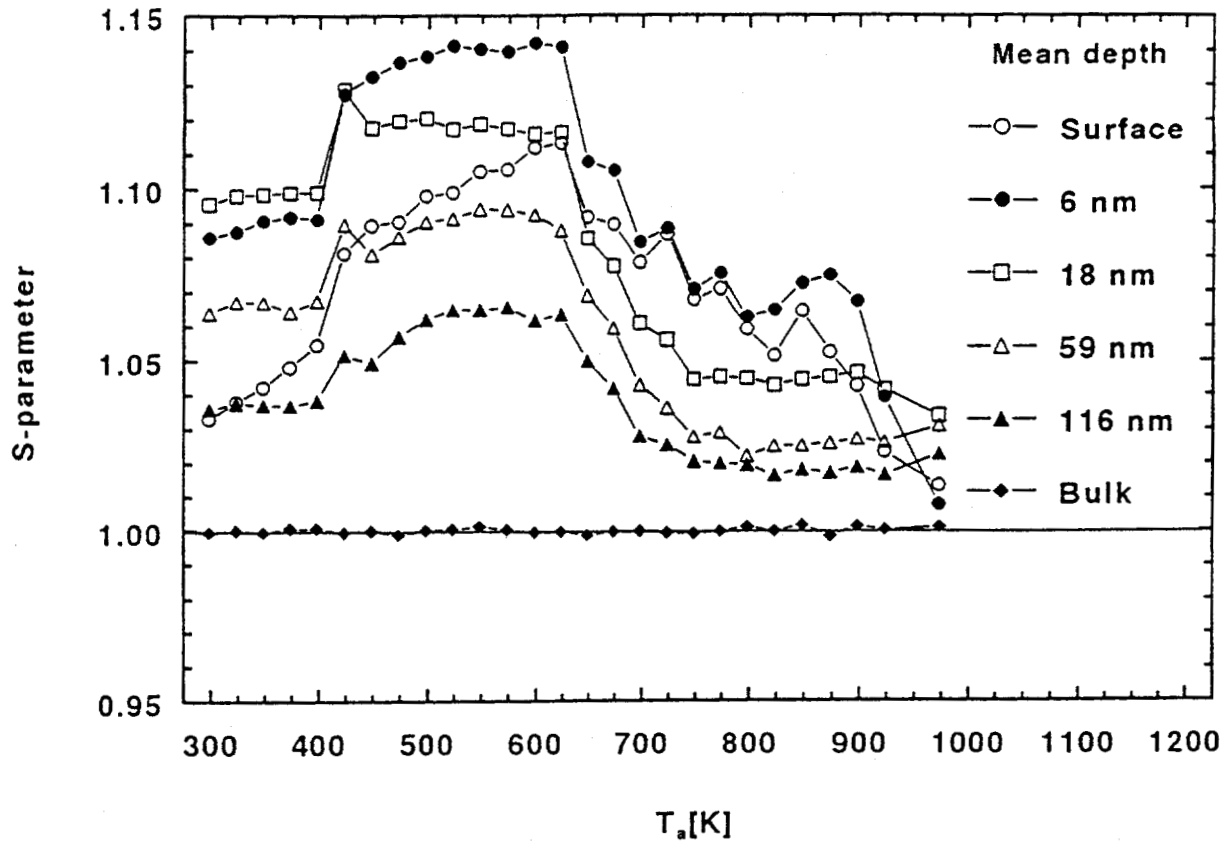


Figure 2. Isochronal anneal experiments for positron-beam depth-profile characterization of specimens Be 4-5 and Be 4-1.

Anneal data, shown in the lower part of Figure 2 for Be 4-1, are different from those shown for Be 4-5. S-parameter data for Be 4-1 are relatively unchanging over a wide temperature range from room temperature to about 775K, at which the values begin to fall indicating the onset of defect annealing. These differences are attributed to the different defect structures created in specimens implanted at different temperatures. Implantation into Be 4-1 at a temperature of 723K resulted in a more stable defect structure (no changes in S-values until 775K) that did not contain any deuterium in low energy trap sites (no rise in S-values at low temperatures). Because of surface-oxide growth during the high temperature anneals, the S-values for the 6-nm and the 36-nm depths extend below the S=1.0 line. These S-parameter data are consistent with a defect structure characterized by a smaller concentration of large voids, as observed in SEM analyses for a similar specimen [4].

In Figure 3, we present additional positron depth-profile data for Be 4-5 during isochronal annealing measurements. A comparison of S-parameter profiles as a function of mean positron energy (and mean positron depth) is made for various anneal conditions. The data show the profile corresponding to 300K (no anneal) and profiles for the specimen subjected to anneals from 623K to 973K. Profiles corresponding to 623K and to 673K appear to contain two components, one located near the surface at 5 nm, and one located deeper, between 20 nm and 40 nm. The deeper component appears to anneal faster than the shallow one. We note that the S-profile for the 973K anneal is shifted to the right because of the influence of a thick oxide layer that developed on the specimen during the high-temperature anneal steps. This effect has also been observed in Al for

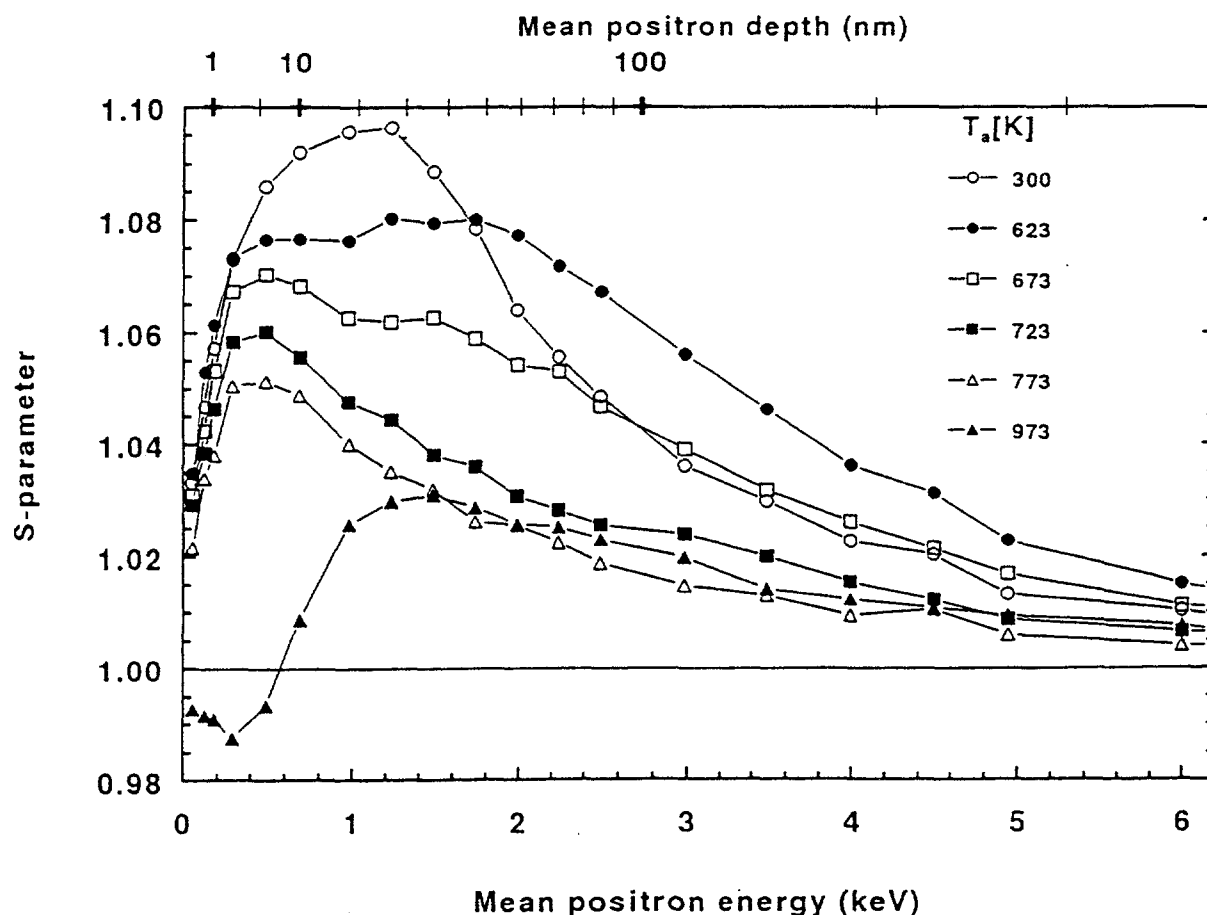


Figure 3. S-parameter depth-profile data for specimen Be 4-5 corresponding to various anneal conditions.

which positron annihilation in the surface oxide resulted in an annihilation-radiation peak with a broader peak shape, hence a smaller S-value [19]. By analytically shifting the S-profile data for the 973K anneal toward the surface, to remove the affect of the oxide layer, we observe that the beryllium foil has a very stable defect structure near the surface. Depth-profile measurements for the backside of the specimen also indicated a near-surface defect structure that was stable to high temperatures.

Evidence of a two-component S-profile distribution was also observed in measurements for specimen Be 4-1, that was implanted at 723K. The near surface component appeared to correspond to that for Be 4-5, in that it peaked at approximately the same positron energy (or depth). However, the second component for Be 4-1 extended further into the bulk and was broader than that for Be 4-5. As we discussed earlier, the broader distribution for Be 4-1 is due to vacancy and deuterium transport associated with implantation into a beryllium at an elevated temperature.

Preliminary analyses were made to derive defect concentrations and defect sizes from the S-parameter data. This analysis was done with VEPFIT[20], a code that models the diffusion/annihilation kinetic equation to fit positron-beam data in which S-parameter measurements are made. Simulation calculations required the use of two defect components to fit the measured data.

Discussion and Conclusions

This work investigated surface material modifications in beryllium due to deuterium implantation at energies ranging from keV to sub-keV, for various specimen temperatures and anneal conditions during the implantation. Positron-beam depth-profile analyses were made to characterize the defect distributions and to develop a better understanding of deuterium ion-induced changes in beryllium and how those changes affect deuterium retention and release.

These analyses identified a varying defect structure in beryllium, dependent on the previous anneal history of the material and on the temperature of the material during implantation with energetic deuterium ions. For unannealed and unimplanted Be, the analyses revealed a deep, broad distribution of vacancy-defect complexes, most likely resulting from foil-fabrication processes. Such defects annealed at temperatures above 473K. A defect structure near the surface was identified in both unimplanted and implanted specimens annealed to 973K. This stable defect structure could be dislocations resulting from foil-fabrication processes. The character and distribution of beam-induced defects in beryllium was highly dependent on the temperature of the material during implantation. For specimens implanted at room temperature with 1-keV/D ions, the beam-induced defect structure had a profile that was peaked near the mean range of the implanting deuterium and that extended beyond the implantation zone. Isochronal step-thermal anneal experiments revealed that deuterium was released from these defects at a temperature of about 400K, indicative of shallow traps, and that the defect structure annealed at temperatures above 623K. These beam-induced vacancy-defect complexes were estimated to be 1-nm voids. For beryllium implanted at temperatures of 723K with 1-keV/D ions, the positron analyses revealed a beam-induced defect structure different from that for specimens implanted at room temperature. In this case, the defect structure was much broader and extended far beyond the implantation zone. Isochronal step-thermal anneal experiments indicated that the defect structure was quite stable, with the onset of defect annealing at 775K. There was no evidence of deuterium release at lower temperatures, indicating that deuterium is retained in deep traps for beryllium implanted at high temperatures. These results, along with previous SEM analyses[4], indicate that, for beryllium implanted at high temperatures, beam-induced defects consist of large, stable voids with concentrations less than those for material implanted at room temperature.

References

1. ITER Conceptual Design, Interim Report, IAEA/ITER/DS/7 (IAEA, Vienna, 1990).
2. K. L. Wilson et al., J. Vac. Sci. Technol. A8(1990) 1750.
3. P. J. Schultz and K. G. Lynn, Rev. Mod. Phys., 60(3)(1988),701.
4. R. A. Anderl et al., J. Nucl. Mater., 196-198 (1992) 986.
5. K. Touhouche and B. Terreault, Mat. Res. Soc. Symp. Proc., 316(1994) 987.
6. B. Terreault, et al., Paper presented at the 11th Inter. Conf. on Plasma Surface Interactions in Controlled Fusion Devices, (1994), to be published J. Nucl. Mater.
7. J. Verbeck and W. Eckstein, in Application of Ion Beams to Metals, eds. S. T. Picraux, E. P. EerNisse and F. L. Vook (Plenum, NY, 1975) 597.
8. M. B. Liu, et al. J. Nucl. Mater., 79 (1979) 267.
9. H. Kawamura et al., J. Nucl. Mater., 176 & 177 (1990) 661.
10. W. R. Wampler, J. Nucl. Mater., 196-198 (1992) 981.
11. W. R. Wampler, J. Nucl. Mater., 122 & 123 (1984) 1598.
12. L. Leblanc and G. G. Ross, Nucl. Inst. and Meth. in Physics Research, B 83 (1993) 15.
13. J. P. Biersack and L. G. Hagmark, Nucl. Inst. and Meth., 174 (1980) 257.
14. D. F. Holland and R. A. Anderl, Fusion Technol., 14(1988)707.
15. R. A. Anderl et al., Fusion Technol., 8(1985)2299.
16. R. W. Siegel, "Positron Annihilation Spectroscopy of Defects in Metals -an Assessment", in Positron Annihilation, P. G. Coleman, S. C. Sharma, L.M. Diana(eds.), (North-Holland Publishing, 1982).
17. B. Nielsen et al., in Positron Annihilation, eds. P. C. Jain, R. M. Singru, and K. P. Gopinathan (World Scientific Publishing, 1985) 497.
18. A. Van Veen, J. of Trace and Microprobe Techniques, 8(1990)1.
19. H. Uomo et al., Appl. Phys. A49(1989) 647.
20. A. Van Veen, et al., AIP Conf Proceedings, Vol 218, (1990)171.